Generation of carrier-envelope-phase-stable 2-cycle 740-μJ pulses at 2.1-μm carrier wavelength

Xun Gu,[1,*] Gilad Marcus,[1] Yunpei Deng,[1] Thomas Metzger,[2] Catherine Teisset,[2] Nobuhisa Ishii,[1,3] Takao Fuji,[1,4] Andrius Baltuska,[1,5] Rytis Butkus,[6] Volodymyr Pervak,[2] Hideki Ishizuki,[7] Takunori Taira,[7] Takayoshi Kobayashi,[8,9] Reinhard Kienberger[1] and Ferenc Krausz[1,2]

[1]*Max-Planck-Institute of Quantum Optics, Hans-Kopfermann-Str. 1, 85748 Garching, Germany*
[2]*Ludwig-Maximilian-Universität München, am Coulombwall 1, 85748 Garching, Germany*
[3]*Currently with Institute for Solid State Physics, University of Tokyo, Kashiwanoha 5-1-5, Kashiwa, Chiba 277-8581, Japan*
[4]*Currently with Chemical Dynamics Laboratory, RIKEN, Hirosawa 2-1, Wako, Saitama 351-0198, Japan*
[5]*Currently with Institute of Photonics, Vienna University of Technology, Vienna, Austria*
[6]*Laser Research Center, Vilnius University, Sauletekio Ave.10, LT-10223 Vilnius, Lithuania*
[7]*Institute for Molecular Science, 38 Nishigonaka, Myodaiji, Okazaki 444-8585, Japan*
[8]*Department of Applied Physics and Chemistry and Institute for Laser Science, University of Electro-Communications, Chofugaoka 1-5-1, Chofu, Tokyo 182-8585, Japan*
[9]*JST, ICORP, Ultrashort Pulse Laser Project, 4-1-8 Honcho, Kawaguchi, Saitama, 332-0012, Japan*
Corresponding author: xun.gu@mpq.mpg.de

Abstract: We produce carrier-envelope-phase-stable 15.7-fs (2-cycle) 740-μJ pulses at the 2.1-μm carrier wavelength, from a three-stage optical parametric chirped-pulse amplifier system, pumped by an optically synchronized 49-ps 11-mJ Nd:YLF laser. A novel seed pulse spectral shaping method is used to ascertain the true amplified seed energy and the parametric superfluorescence levels.

©2008 Optical Society of America

References and links

1. P. B. Corkum and F. Krausz, "Attosecond science," Nature Phys. **3**, 381-387 (2007).
2. E. Goulielmakis, V. S. Yakovlev, A. L. Cavalieri, M. Uiberacker, V. Pervak, A. Apolonski, R. Kienberger, U. Kleineberg, and F. Krausz, "Attosecond Control and Measurement: Lightwave Electronics," Science **317**, 769-775 (2007).
3. I. P. Christov, M. M. Murnane, and H. C. Kapteyn, "High-Harmonic Generation of Attosecond Pulses in the "Single-Cycle" Regime," Phys. Rev. Lett. **78**, 1251 (1997).
4. J. L. Krause, K. J. Schafer, and K. C. Kulander, "High-order harmonic generation from atoms and ions in the high-intensity regime," Phys. Rev. Lett. **68**, 3535-3538 (1992).
5. P. Colosimo, G. Doumy, C. I. Blaga, J. Wheeler, C. Hauri, F. Catoire, J. Tate, R. Chirla, A. M. March, G. G. Paulus, H. G. Muller, P. Agostini, and L. F. Dimauro, "Scaling strong-field interactions towards the classical limit," Nature Phys. **4**, 386-389 (2008).
6. J. Tate, T. Auguste, H. G. Muller, P. Salieres, P. Agostini, and L. F. DiMauro, "Scaling of wave-packet dynamics in an intense midinfrared field," Phys. Rev. Lett. **98** (2007).
7. A. Gordon and F. X. Kärtner, "Scaling of keV HHG photon yield with drive wavelength," Opt. Express **13**, 2491-2497 (2005).
8. V. S. Yakovlev, M. Ivanov, and F. Krausz, "Enhanced phase-matching for generation of soft X-ray harmonics andattosecond pulses in atomic gases," Opt. Express **15**, 15351-15364 (2007).
9. O. Isaienko and E. Borguet, "Generation of ultra-broadband pulses in the near-IR by non-collinear optical parametric amplification in potassium titanyl phosphate," Opt. Express **16**, 3949-3954 (2008).
10. C. Vozzi, G. Cirmi, C. Manzoni, E. Benedetti, F. Calegari, G. Sansone, S. Stagira, O. Svelto, S. De Silvestri, M. Nisoli, and G. Cerullo, "High-energy, few-optical-cycle pulses at 1.5 μm with passive carrier-envelope phase stabilization," Opt. Express **14**, 10109-10116 (2006).
11. C. Vozzi, F. Calegari, E. Benedetti, S. Gasilov, G. Sansone, G. Cerullo, M. Nisoli, S. De Silvestri, and S. Stagira, "Millijoule-level phase-stabilized few-optical-cycle infrared parametric source," Opt. Lett. **32**, 2957-2959 (2007).
12. D. Brida, G. Cirmi, C. Manzoni, S. Bonora, P. Villoresi, S. De Silvestri, and G. Cerullo, "Sub-two-cycle light pulses at 1.6 μm from an optical parametric amplifier," Opt. Lett. **33**, 741-743 (2008).

13. C. P. Hauri, R. B. Lopez-Martens, C. I. Blaga, K. D. Schultz, J. Cryan, R. Chirla, P. Colosimo, G. Doumy, A. M. March, C. Roedig, E. Sistrunk, J. Tate, J. Wheeler, L. R. DiMauro, and E. P. Power, "Intense self-compressed, self-phase-stabilized few-cycle pulses at 2 µm from an optical filament," Opt. Lett. **32**, 868-870 (2007).
14. C. J. Fecko, J. J. Loparo, and A. Tokmakoff, "Generation of 45 femtosecond pulses at 3 µm with a KNbO3 optical parametric amplifier," Opt. Commun. **241**, 521-528 (2004).
15. O. D. Mücke, D. Sidorov, P. Dombi, A. Pugzlys, A. Baltuska, S. Alisauskas, J. Pocius, L. Giniunas, and R. Danielius, "Multimillijoule Optically Synchronized and Carrier-Envelope-Phase-Stable Chirped Parametric Amplification at 1.5 µm," in XVI International Conference on Ultrafast Phenomena(European Physical Society, Streas (Lago Maggiore), Italy, 2008).
16. T. Fuji, N. Ishii, C. Y. Teisset, X. Gu, T. Metzger, A. Baltuska, N. Forget, D. Kaplan, A. Galvanauskas, and F. Krausz, "Parametric amplification of few-cycle carrier-envelope phase-stable pulses at 2.1 µm," Opt. Lett. **31**, 1103-1105 (2006).
17. A. Dubietis, G. Jonusauskas, and A. Piskarskas, "Powerful femtosecond pulse generation by chirped and stretched pulse parametric amplification in BBO crystal," Opt. Commun. **88**, 437-440 (1992).
18. I. N. Ross, P. Matousek, M. Towrie, A. J. Langley, and J. L. Collier, "The prospects for ultrashort pulse duration and ultrahigh intensity using optical parametric chirped pulse amplifiers," Opt. Commun. **144**, 125-133 (1997).
19. A. Baltuska, T. Fuji, and T. Kobayashi, "Controlling the Carrier-Envelope Phase of Ultrashort Light Pulses with Optical Parametric Amplifiers," Phys. Rev. Lett. **88**, 133901 (2002).
20. T. Fuji, A. Apolonski, and F. Krausz, "Self-stabilization of carrier-envelope offset phase by use of difference-frequency generation," Opt. Lett. **29**, 632-634 (2004).
21. G. Cirmi, C. Manzoni, D. Brida, S. De Silvestri, and G. Cerullo, "Carrier-envelope phase stable, few-optical-cycle pulses tunable from visible to near IR," J. Opt. Soc. Am. B **25**, B62-B69 (2008).
22. C. Manzoni, C. Vozzi, E. Benedetti, G. Sansone, S. Stagira, O. Svelto, S. De Silvestri, M. Nisoli, and G. Cerullo, "Generation of high-energy self-phase-stabilized pulses by difference-frequency generation followed by optical parametric amplification," Opt. Lett. **31**, 963-965 (2006).
23. N. Ishii, C. Y. Teisset, T. Fuji, S. Kohler, K. Schmid, L. Veisz, A. Baltuska, and F. Krausz, "Seeding of an eleven femtosecond optical parametric chirped pulse amplifier and its Nd3+ picosecond pump laser from a single broadband Ti:Sapphire oscillator," IEEE J. Sel. Top. Quantum Electron. **12**, 173-180 (2006).
24. H. Ishizuki and T. Taira, "High-energy quasi-phase-matched optical parametric oscillation in a periodically poled MgO:LiNbO3 device with a 5 mm × 5 mm aperture," Opt. Lett. **30**, 2918-2920 (2005).
25. Y.-H. Cha, Y.-W. Lee, S. M. Nam, J. M. Han, Y. J. Rhee, B. D. Yoo, B. C. Lee, and Y. U. Jeong, "Simple method for the temporal characterization of amplified spontaneous emission in femtosecond terawatt Ti:sapphire lasers," Appl. Opt. **46**, 6854-6858 (2007).
26. T. Tsang, M. A. Krumbugel, K. W. DeLong, D. N. Fittinghoff, and R. Trebino, "Frequency-resolved optical-gating measurements of ultrashort pulses using surface third-harmonic generation," Opt. Lett. **21**, 1381-1383 (1996).

1. Introduction

Isolated attosecond pulses of photon energies up to ~100 eV can now be routinely generated and utilized in a host of interesting applications requiring atomic time resolutions, creating an entire new field of attosecond physics [1]. Typically, such pulses are generated by high-harmonic generation (HHG) in a noble gas, driven by intense few-cycle laser pulses provided by a Ti:sapphire laser amplifier system at a wavelength around 800 nm [2, 3].

The cutoff energy in the high-harmonic spectrum is given in atomic units by the formula $I_p + 3.17 U_p$, where I_p is the atom's ionization potential, and $U_p = E^2 / 4\omega^2$ is the ponderomotive potential, where E is the driver laser's field strength, and ω is the frequency [4]. It has been suggested and recently demonstrated [5] that using a long-wavelength driver, coherent x-ray photon energy cutoff can be significantly extended. The wavelength-scaling law of the HHG yield remains an interest of theoretical investigation [6, 7], and a recent paper shows that favorable phase-matching can be realized for mid-IR drivers [8]. Several efforts have been reported so far on the development of high-intensity few-cycle IR optical parametric amplifiers (OPA) working at wavelengths around 1.2 µm [9], 1.5 µm [10-12], 2 µm [13] and 3 µm [14], pumped by Ti:sapphire amplifier systems, and in a 1.5-µm system [15], pumped by a combination of Yb and Nd amplifiers. In 2006, we demonstrated a 1-kHz carrier-envelope-phase (CEP) stable 20-fs 2.1-µm-carrier-wavelength system, generating ~80 µJ pulses with a well-suppressed parametric superfluorescence background [16], pumped by a
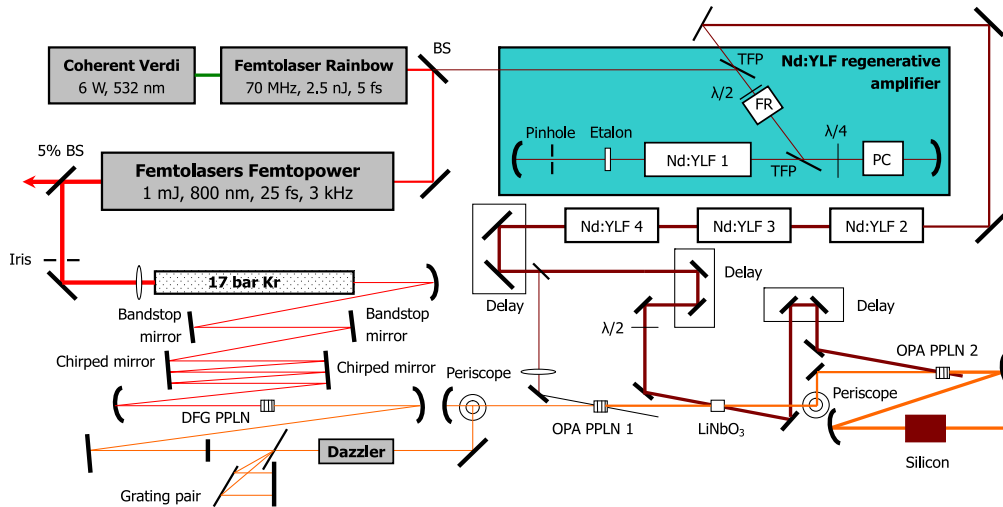
Fig. 1. Schematic of the mid-IR OPCPA system.

Nd:YLF laser system, using the concept of optical parametric chirped-pulse amplification (OPCPA) [17, 18]. In this Letter, we report the latest upgrade of this system to an output of CEP-stable 15.7-fs (2-optical-cycle), 740-µJ pulses, which are the shortest sub-mJ pulses ever generated at this spectral range. A novel method of seed pulse shaping is used to ascertain the true amplified signal energy, solving a long-standing practical issue in high gain OPA development. This system will be an ideal driver for HHG of coherent x-ray photons in the keV regime.

2. System description

The schematic of the upgraded OPCPA system is shown in Fig. 1. A major problem with the previously reported system was the high superfluorescence background due to the low IR seed pulse energy, limiting the amount of useful amplified signal. In the current system, 5% of the
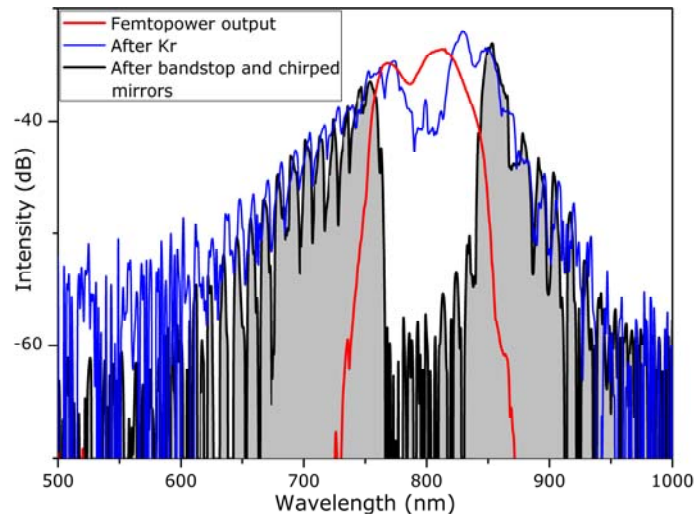

Fig. 2. Spectra of the Femtopower Pro laser system output pulse (red), the spectrally broadened pulse after the krypton cell (blue), and the pulse after the bandstop and chirped mirrors (black).

1-mJ 25-fs output of a 3-kHz Femtopower Pro Ti:sapphire multipass amplifier is first spatially clipped by an iris, reducing the pulse energy to 12.3 µJ, and then focused into a gas cell filled with 17-bar krypton, where the pulse creates a single filament which broadens its spectrum to cover a spectral range from ~600 to ~950 nm. The spectrally broadened pulse is then filtered to remove the strong central part of the spectrum by homemade bandstop mirrors (in order to avoid damage or photorefraction in the DFG crystal), and afterwards temporally compressed by chirped mirrors. The bandstop mirrors are designed so to have flat dispersion and uniform reflectivity in the spectral regions below 750 nm and above 850 nm. The low and the high-frequency wings of the pulse spectrum are subsequently mixed in a 1-mm-long MgO-doped periodically poled LiNbO$_3$ crystal (PPMgLN) with a 11.21-µm poling period, generating a difference-frequency signal from 1.7 to 2.6 µm. The spectra of the Ti:sapphire pulse, the spectrally broadened pulse after the krypton cell, and the pulse after the bandstop and chirped mirrors, are shown in Fig. 2. The difference-frequency generation (DFG) scheme ensures the CEP stability of the IR pulse [19, 20], which is faithfully preserved in the subsequent OPA processes, as shown by previous investigations in our system [16] and in other OPA systems [10, 11, 13, 21, 22]. The IR seed pulse energy is estimated to be a few nJ, significantly higher than the 4 pJ level in the previous report, which directly used the output of a Ti:sapphire oscillator for the DFG.

Our pump laser is a Nd:YLF amplifier chain, consisting of a regenerative amplifier and three linear post-amplifiers, all developed in house [23]. It is seeded by the Ti:sapphire oscillator (Femtolasers Rainbow) which also seeds the Femtopower system, whose spectrum extends just beyond ~1060 nm. The oscillator output pulse energy within the fluorescence bandwidth of Nd:YLF at 1053 nm is measured to be ~2 pJ. The regenerative amplifier, using a Northrop-Grumman laser module containing a 80-mm-long 4-mm-diameter a-cut Nd:YLF rod, amplifies the pulse to 3.7 mJ at a 1 kHz repetition rate, and the three linear post-amplifier modules containing 120-mm-long 4-mm-diameter a-cut Nd:YLF rods, further amplify the pulse to 11 mJ. The pulse energy stability is measured to be 1.2% rms. A third-order autocorrelation measurement of the pump laser system output puts the intensity contrast ratio between the peak of the amplified pulse and the amplified spontaneous emission (ASE) floor at 10^3. The FWHM pulse duration, assuming a Gaussian pulse shape, is 49 ps.

Three near-degenerate OPA stages are used in our system, in which the seed and the idler pulses are of the same wavelength, thus providing a broad amplification bandwidth. The signal and the pump beams are crossed at a small angle (~3°) to spatially separate them and to avoid signal-idler interference. A beamsplitter splits off 3% of the pump beam to the first-stage OPA, which employs a 3-mm-thick PPMgLN crystal with a 30.2-µm poling period (HC Photonics), heated to 280°C to minimize the parasitic photorefractive effect. The amplified seed pulse and the remaining 97% of the pump beam are combined in the second-stage OPA
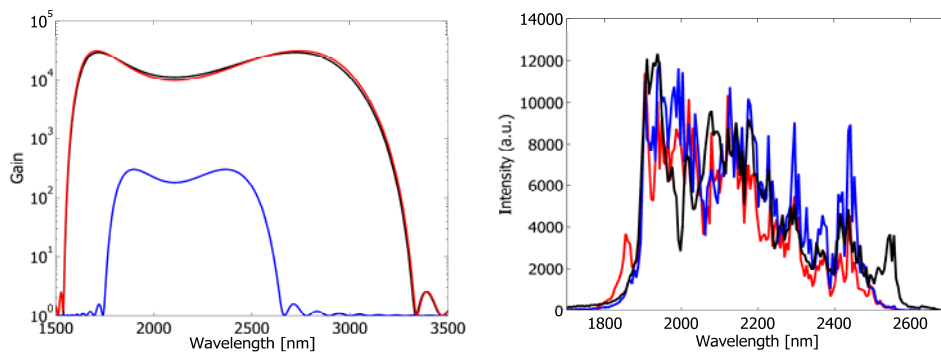

Fig. 3. Left: Calculated unsaturated gain profiles of the first (black), second (blue) and third (red) OPA stages. Right: Amplified pulse spectra of the first (red), the second (blue) and the third (black) OPA stages.

of a 4-mm-thick type-I LiNbO$_3$ crystal, and again in the third-stage OPA of a 3-mm-thick PPMgLN crystal of a 30.6-μm poling period, heated to 120°C. The third-stage PPMgLN crystal, manufactured by the Institute of Molecular Science in Japan, has an extraordinarily large aperture of 5 mm × 5 mm [24], allowing us to use a large beam size (FWHM 1.5 mm) to alleviate optical damage concerns in the crystal. Nevertheless, to avoid detrimental photorefraction-induced beam distortion, it is necessary to use a narrower-bandwidth bulk LiNbO$_3$ amplifier in the second stage to pre-amplify the IR pulse, before finally boosting the output pulse energy and broadening the gain bandwidth in the final PPMgLN crystal. The OPA system output, including possible superfluorescence, is 6 μJ after the first stage, 200 μJ after the second stage, and 920 μJ after the third stage. The energy stability of the third-stage output is 9% rms. The beam profile is very good, as shown in the inset of Fig. 4. The calculated OPA gain profiles and the measured spectra of the amplified pulse in each stage are shown in Fig. 3.

In order to extract the maximum energy from the pump, the IR seed pulse should be stretched to match its duration to that of the pump pulse as closely as possible. Compared to the previous system in which a Fastlite Dazzler acousto-optic pulse shaper alone was used to stretch the seed pulse to ~10 ps, the current version employs an additional 300 line/mm grating pair, which are separated by 75 mm along the beam with a 30° incidence angle. In combination with the Dazzler, the seed pulse is stretched to ~25 ps. The amplified IR pulse is recompressed by a 100-mm-long silicon block. High-quality pulse compression to near the Fourier limit is achieved by fine-tuning the Dazzler phase, which can take the form of an arbitrary curve within its tuning range.

3. Determining true levels of amplified signal and superfluorescence

Despite the significant improvement in the seed energy, parametric superfluorescence still constitutes a considerable portion of the pulse energy in the final OPA output. Indeed, with the IR seed beam blocked, the combined three OPA stages produce a superfluorescence level
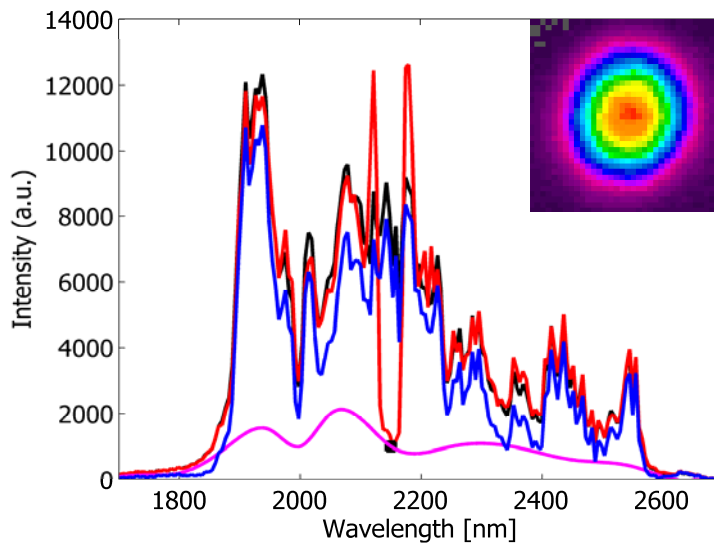

Fig. 4. Spectra of the full third-stage OPA output (black), the OPA output with a 50-nm-wide Dazzler-imposed spectral hole at 2150 nm (red), the superfluorescence profile traced out by hole depths at different wavelengths (magenta), and the true amplified signal (blue, the full OPA output minus the superfluorescence). The black square denotes the measured level of superfluorescence at 2150 nm by the spectral hole technique. Inset: Beam profile of the third-stage OPA output 20 cm after the crystal.

of ~780 µJ, almost equal to that of the full amplified signal with an unblocked seed. However, it is important to note that, with the pump pulse energy significantly depleted in the final OPA stage, the superfluorescence in the seed-unblocked case can be much smaller than in the seed-blocked case. That is because, with an unblocked seed beam, both the seed pulse and the noise that initiates the superfluorescence experience the same saturated parametric gain, whereas with the seed beam blocked, the noise experiences a much higher unsaturated gain. Therefore, ascertaining the true amplified signal and the superfluorescence levels in a high-gain low-seed OPA system remains so far an unsolved thorny issue in the current OPA research.

To resolve this issue, we have employed a novel method of seed pulse spectral shaping. In the absence of superfluorescence, any shaping of the IR seed spectrum by the Dazzler will be directly transferred to the amplified signal. In particular, if we annihilate a narrow region in the seed spectrum (or to create a zero-reaching spectral "hole") using the Dazzler, the real amplified seed will preserve the spectral hole with a 100% modulation depth. (A spectral hole can also be created by placing a narrow object on the Fourier plane within the grating stretcher. This method produces the same result as the Dazzler pulse-shaping.) Broadband parametric superfluorescence, on the other hand, is not shaped and its level unchanged if the hole is narrow enough. Therefore, in the combined spectrum, the spectral hole will be partially refilled by the superfluorescence. By measuring the depth of the spectral hole at different wavelengths across the spectrum, we can trace out the superfluorescence spectral distribution relative to the full OPA output, and determine how much energy is in the superfluorescence and in the amplified signal, respectively. It should be noted that a similar method based on the same principle has been recently used in estimating the ASE level in a Ti:sapphire amplifier system, albeit in the time domain using a fast photodiode [25].

Let us now have a brief discussion on the basic assumptions and limitations of this simple superfluorescence estimation method. First of all, it's easy to see that for this method to work, the seed pulse should be heavily chirped in the OPA crystals, so much so that its temporal profile faithfully reflects its spectral shape. Only then will a sharp and narrow hole in the seed spectrum be turned into a sharp and narrow gap in its temporal profile. Under this condition, the superfluorescence level outside the narrow temporal gap in the seed pulse will not be affected by the shaping of the seed pulse. In our system, the seed pulse of more than 800 nm bandwidth is stretched to ~25 ps, comfortably satisfying this condition. Secondly, the superfluorescence inside the temporal gap created in the seed pulse will become stronger at the unsaturated level because no seed is present there to deplete the pump. Therefore, the temporal gap, or the spectral hole, in the seed pulse should be made narrow enough to avoid overestimation of the superfluorescence. In our measurement, we used a 50-nm wide spectral hole, about 6% of the total bandwidth. We have also tried holes of varying widths, and confirmed that the choice of the hole width up to 100 nm did not change of the depth of the hole in our measurement.

We have used this simple method to measure the superfluorescence in our OPA system output, and the result is presented in Fig. 4. From this measurement, it is clear that out of the total 920 µJ third-stage OPA output, 740 µJ (80%) belongs to the amplified seed and the rest (20%) belongs to the superfluorescence. In comparison, the superfluorescence is negligible in the first-stage OPA output, and accounts for 2.5% of the second-stage OPA output.

4. Pulse characterization

The final compressed output pulse of the OPCPA system is characterized by a third-harmonic-generation (THG) frequency-resolved optical gating (FROG) [26] apparatus. The third-harmonic signal is generated on an air-CaF_2 interface, which possesses a large bandwidth sufficient to cover the full bandwidth of the amplified IR signal. A home-written FROG retrieval code is used to retrieve the pulse intensity and phase from the measured THG FROG trace. Several iterations have been used to make fine spectral phase corrections with the Dazzler using the result of the FROG retrieval, ultimately making the compressed pulse approach the Fourier-transform limit as closely as possible. The THG FROG measurement
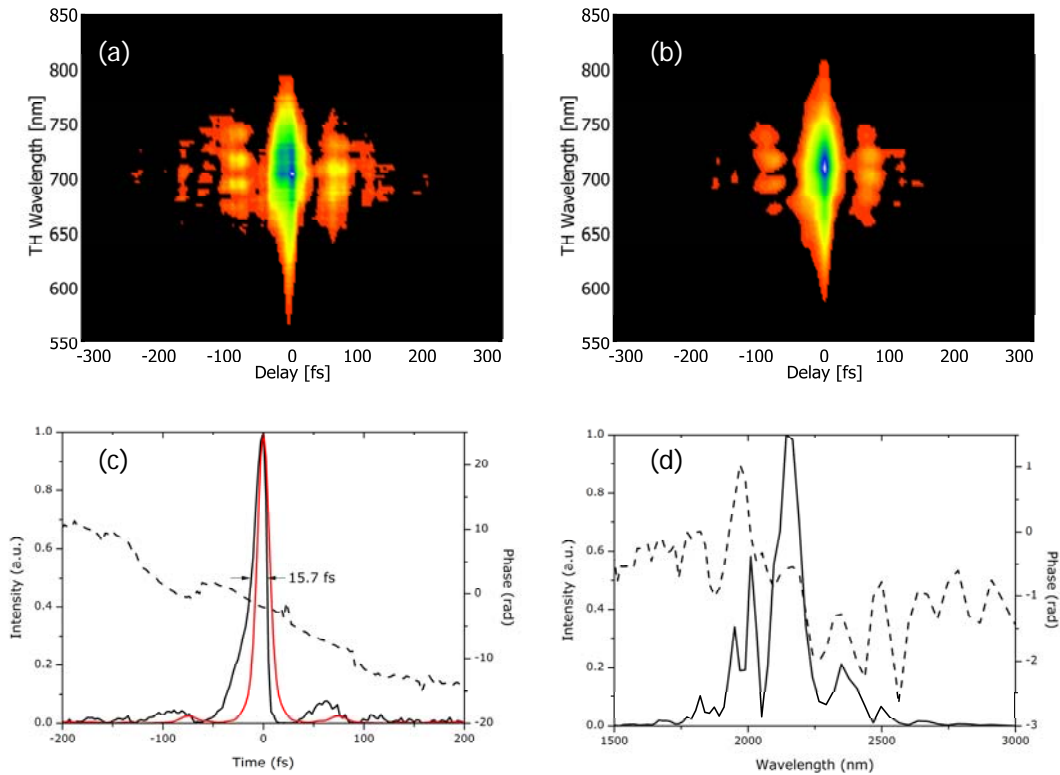
Fig. 5. THG FROG measurement results of the compressed 15.7-fs pulse. (a) Measured FROG trace, (b) retrieved FROG trace, (c) temporal intensity and phase, (d) spectral intensity and phase. The black and the red curves in (c) are the measured and the ideal Fourier-limit intensity profiles, respectively.

results of the final compressed pulse are presented in Fig. 5. The temporal intensity profile of the compressed pulse measures a FWHM of 15.7 fs, which is very close to the Fourier limit of 14.6 fs. At 2.1 μm, this pulse duration corresponds to merely 2 optical cycles. This is, to our knowledge, the shortest sub-mJ level pulse ever generated at this wavelength.

The compression ratio of 25 ps to 15.7 fs and the amplified signal to superfluorescence energy ratio of ~2:1 means that the intensity contrast between the compressed amplified signal pulse and the parametric superfluorescence is larger than 10^3, which should be sufficient for a high-quality HHG experiment. Furthermore, as shown in the previously reported f-to-3f nonlinear interferometry measurement [16], the CEP of the amplified signal is stable, which is also important for HHG.

5. Conclusion

In conclusion, we report the generation of 2-cycle (15.7-fs), 740-μJ pulse at the carrier wavelength of 2.1 μm and the repetition rate of 1 kHz, from a broadband OPCPA system. A novel method of seed spectral shaping is used to solve the nontrivial problem of determining the true superfluorescence level and the amplified signal energy from the total pulse energy of 920 μJ.

Acknowledgments